Figures and figure supplements

Rab5 and Rab11 maintain hematopoietic homeostasis by restricting multiple signaling pathways in *Drosophila*

Shichao Yu *et al*

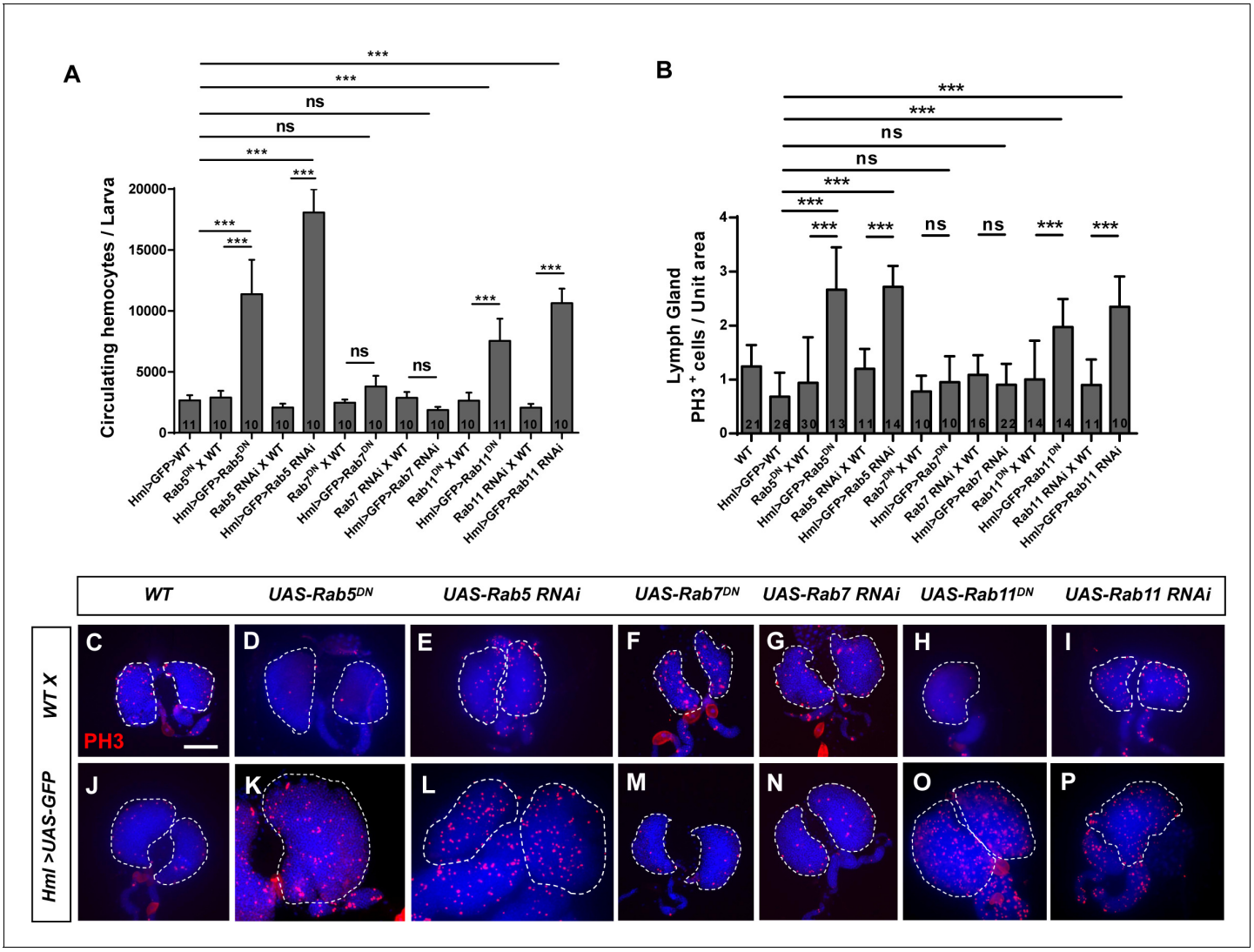

Figure 1. Inhibiting *Rab5* or *Rab11* promoted cell proliferation in circulating hemocytes and lymph glands. (**A**) The number of circulating hemocytes increased upon the loss of *Rab5* or *Rab11* but not *Rab7* in hemocytes. (**B–P**) Immunostaining for PH3 was performed in lymph glands from third instar larvae. The number of PH3-positive cells increased after the inactivation of *Rab5* or *Rab11* but not *Rab7*. The PH3-positive cell count per unit area was calculated as the PH3-positive cell count on a single anterior lobe divided by the area of the single anterior lobe; the quantification is shown in (**B**). Scale bar: 50 μm. ns, not significant; ***p<0.001 (one-way ANOVA).

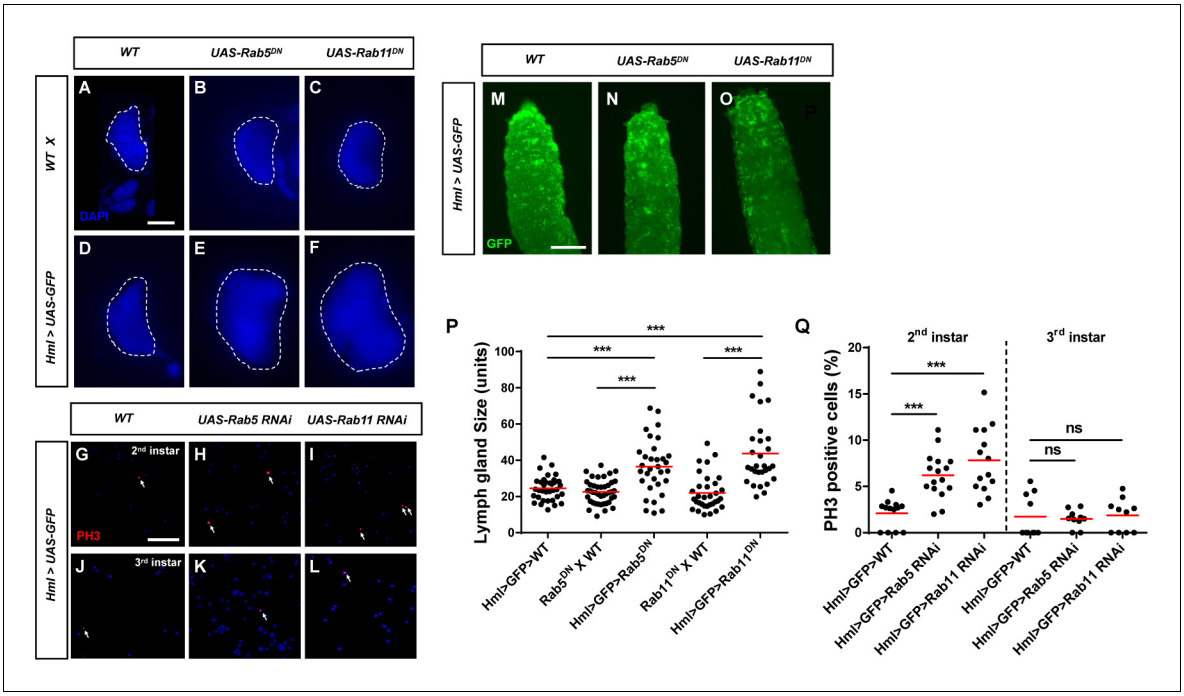

Figure 1—figure supplement 1. Analyses of lymph gland size and cell proliferation in circulating hemocytes as well as the sessile hemocyte pattern. (**A–F, P**) Lymph glands were labeled with DAPI to measure the anterior lobe area. The anterior lobe areas in different genotypes are shown in (**P**). (**G–L, Q**) Cell proliferation was analyzed in hemocytes from second instar (**G–I**) and third instar larvae (**J–L**) via anti-PH3 antibodies, and the PH3-positive cell percentage is shown in (**Q**). (**M–O**) The sessile hemocyte pattern was unchanged in *Hml>UAS-Rab5/11^{DN}* larvae. Scale bars: 50 μm (lymph glands and hemocytes) and 500 μm (larvae). ns, not significant; ***p<0.001 (one-way ANOVA).

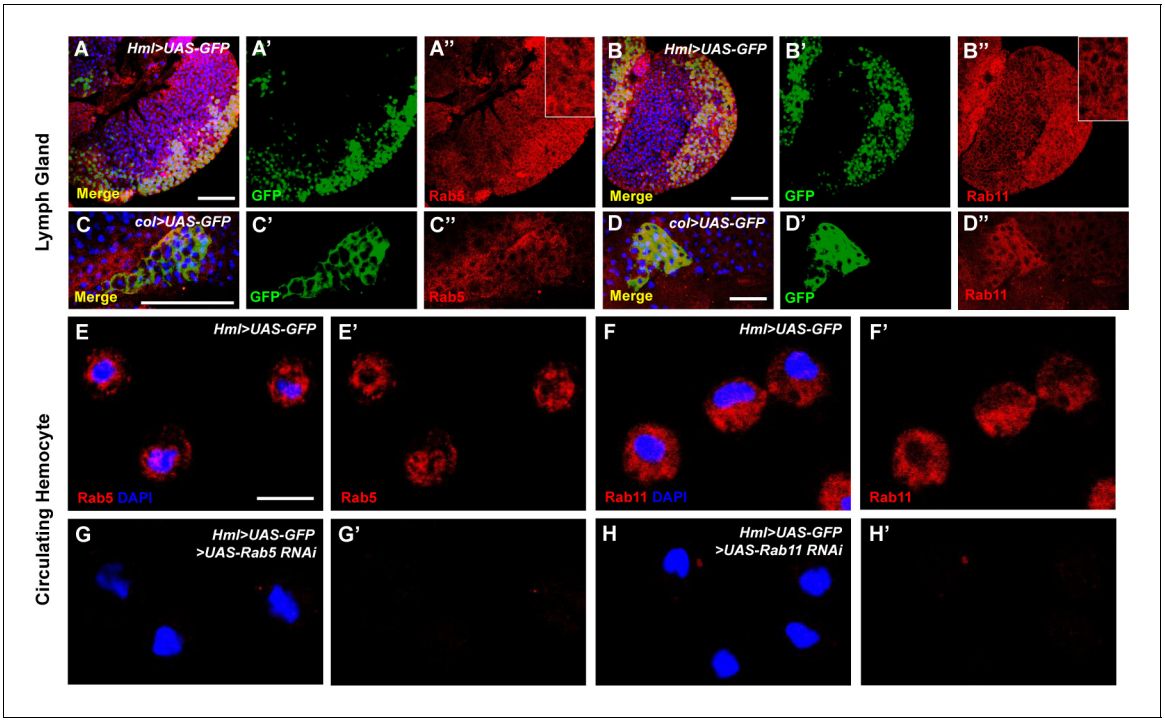

Figure 1—figure supplement 2. Localization of the Rab5 and Rab11 proteins in lymph glands and hemocytes. (**A–D''**) The localization of Rab5 and Rab11 was analyzed in *Hml>UAS-GFP* and *col>UAS-GFP* lymph glands with anti-GFP (green) and anti-Rab5 (red) or anti-Rab11 (red) antibodies as appropriate. (**E–H'**) No Rab5 or Rab11 signals were observed in *Hml>UAS-GFP>UAS-Rab5 RNAi* or *Hml>UAS-GFP>UAS-Rab11 RNAi* hemocytes, respectively. Scale bars: 10 μm (hemocytes) and 50 μm (lymph glands).

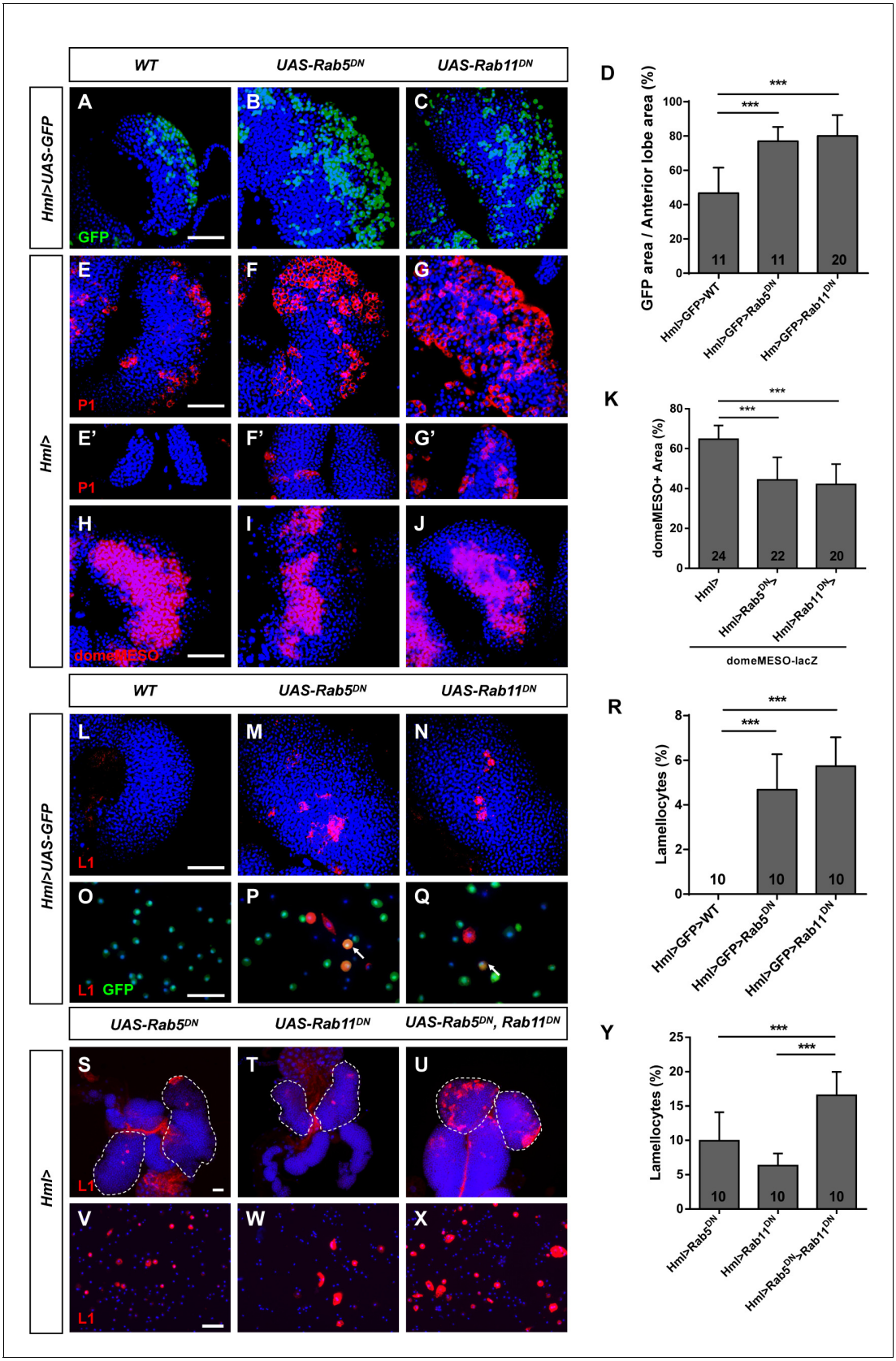

Figure 2. Inactivation of *Rab5* or *Rab11* promoted differentiation in circulating hemocytes and lymph glands. (**A–D**) The percentage of the GFP-positive area in anterior lobes was increased in *Hml>UAS-GFP>UAS-Rab5^{DN}* and *Hml>UAS-GFP>UAS-Rab11^{DN}* lymph glands; the quantification is shown in (**D**).

Figure 2 continued on next page

Figure 2 continued

(**E–G'**) Immunostaining for the plasmatocyte marker P1 showed that the P1-positive area was increased upon the inactivation of *Rab5* or *Rab11* in both the anterior (**E–G**) and posterior lobes (**E'–G'**). (**H–K**) Analysis using the medullary zone (MZ) marker *domeMESO-lacZ* showed that the MZ area was decreased in *Hml>UAS-Rab5^{DN}* and *Hml>UAS-Rab11^{DN}* lymph glands. The proportion of the MZ area in the anterior lobe is shown in (**K**). (**L–Y**) Immunostaining for the lamellocyte marker L1 showed that the lamellocyte count was increased in lymph glands (**L–N**) and circulating hemocytes (**O–Q**) when Rab5 or Rab11 GTPase activity was disrupted. Aberrant lamellocyte differentiation was more severe in lymph glands (**S–U**) and circulating hemocytes (**V–X**) after the simultaneous disruption of Rab5 and Rab11. The lamellocyte frequency among total circulating hemocytes is shown in (**R**) and (**Y**). Scale bar: 50 μm. ***p<0.001 (one-way ANOVA).

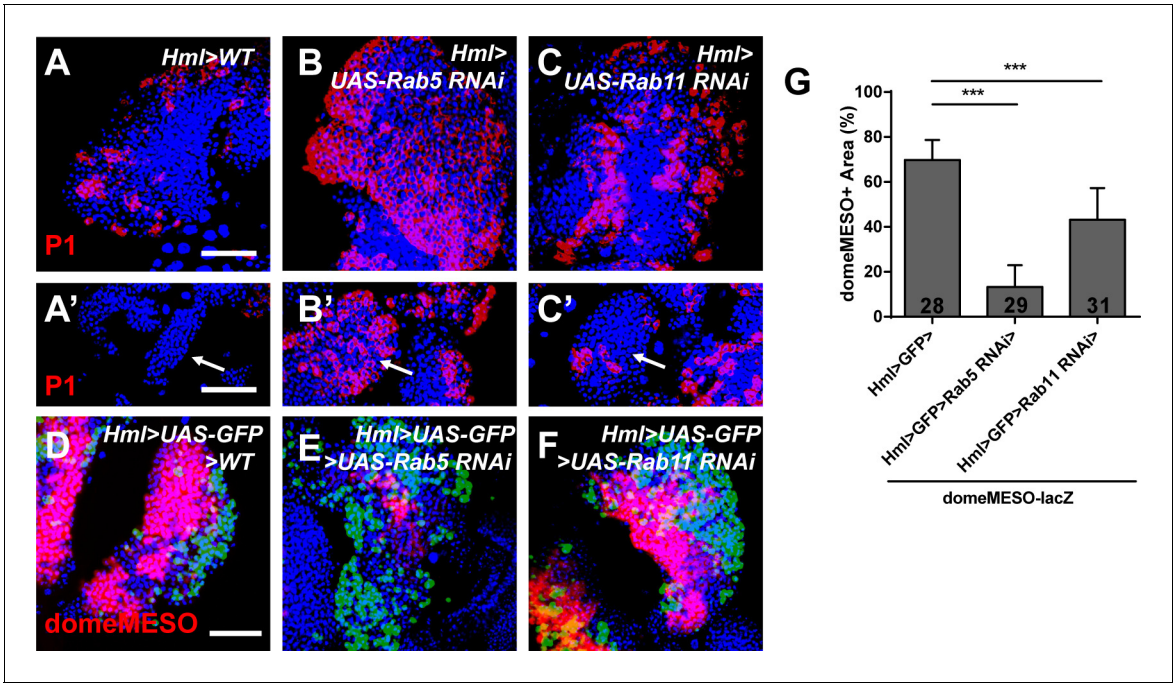

Figure 2—figure supplement 1. Evaluation of the plasmatocyte count and medullary zone (MZ) area in the lymph gland after *Rab5*/*Rab11* inactivation. (**A–C'**) The plasmatocyte count was increased in the anterior (**A–C**) and posterior (**A'–C'**) lobes in lymph glands from *Hml>UAS-Rab5 RNAi* and *Hml>UAS-Rab11 RNAi* larvae, as determined by anti-P1 immunostaining. The arrows show the posterior lobes. (**D–G**) The MZ area was measured in *Hml>UAS-GFP>domeMESO-lacZ*, *Hml>UAS-GFP>UAS-Rab5 RNAi>domeMESO-lacZ*, and *Hml>UAS-GFP>UAS-Rab11 RNAi>domeMESO-lacZ* lymph glands; the quantification is shown in (**G**). Scale bar: 50 μm. ***p<0.001 (one-way ANOVA).

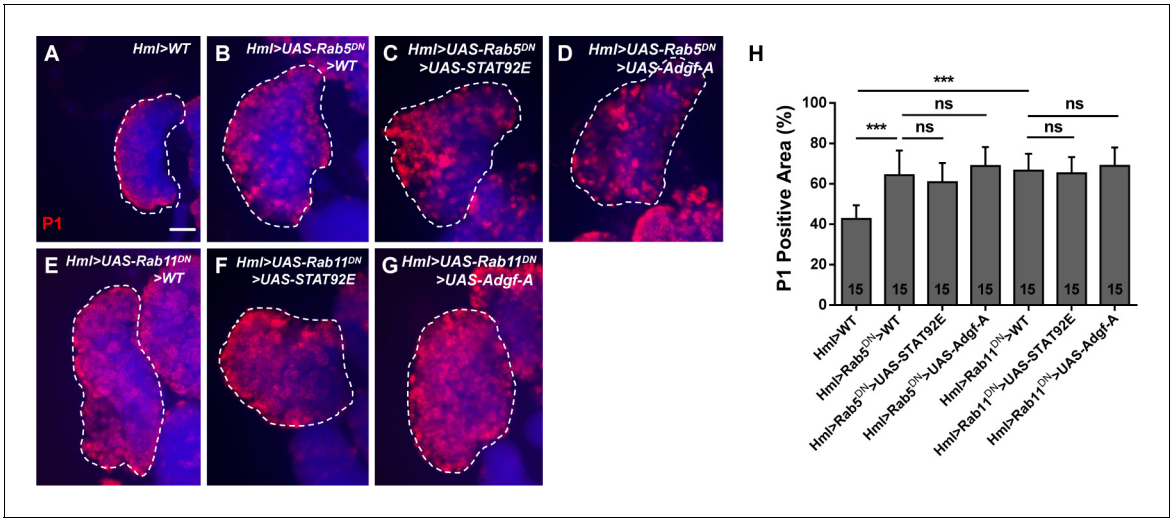

Figure 2—figure supplement 2. Overexpression of *STAT92E* or *Adgf-A* did not rescue the increased P1-positive area in *Hml>UAS-Rab5/11^{DN}* lymph glands. (**A–H**) P1 staining was performed in *Hml>WT* (**A**), *Hml>UAS-Rab5/11^{DN}>WT* (**B, E**), *Hml>UAS-Rab5/11^{DN}>UAS-STAT92E* (**C, F**), and *Hml>UAS-Rab5/11^{DN}>UAS-Adgf-A* (**D, G**) lymph glands. The quantifications of the proportions of P1-positive areas are shown in (**H**). Scale bar: 50 μm. ns, not significant; ***p<0.001 (one-way ANOVA).

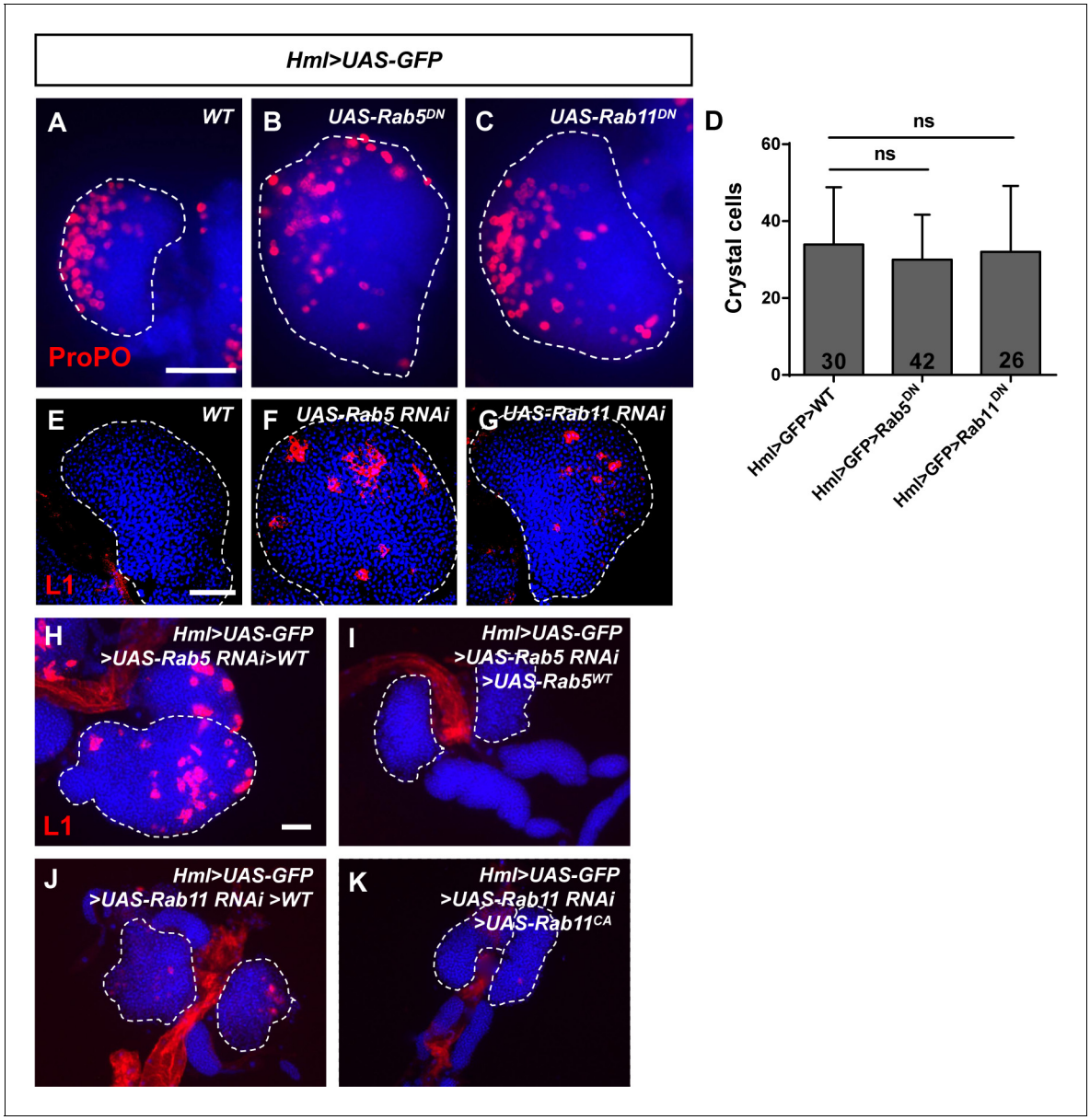

Figure 2—figure supplement 3. Analysis of the crystal cell count and rescue assays of lamellocyte differentiation in lymph glands. (**A–D**) The crystal cell count (as evaluated by anti-ProPO staining) was unchanged in lymph glands upon the inactivation of *Rab5* or *Rab11*. (**E–G**) Aberrant lamellocyte formation was observed in *Hml>UAS-GFP>UAS-Rab5/11 RNAi* lymph glands. (**H–K**) The aberrant lamellocyte differentiation was rescued in *Hml>UAS-GFP>UAS-Rab5 RNAi>UAS-Rab5^{WT}* and *Hml>UAS-GFP>UAS-Rab11 RNAi>UAS-Rab11^{CA}* lymph glands. ns, not significant. Scale bar: 50 μm.

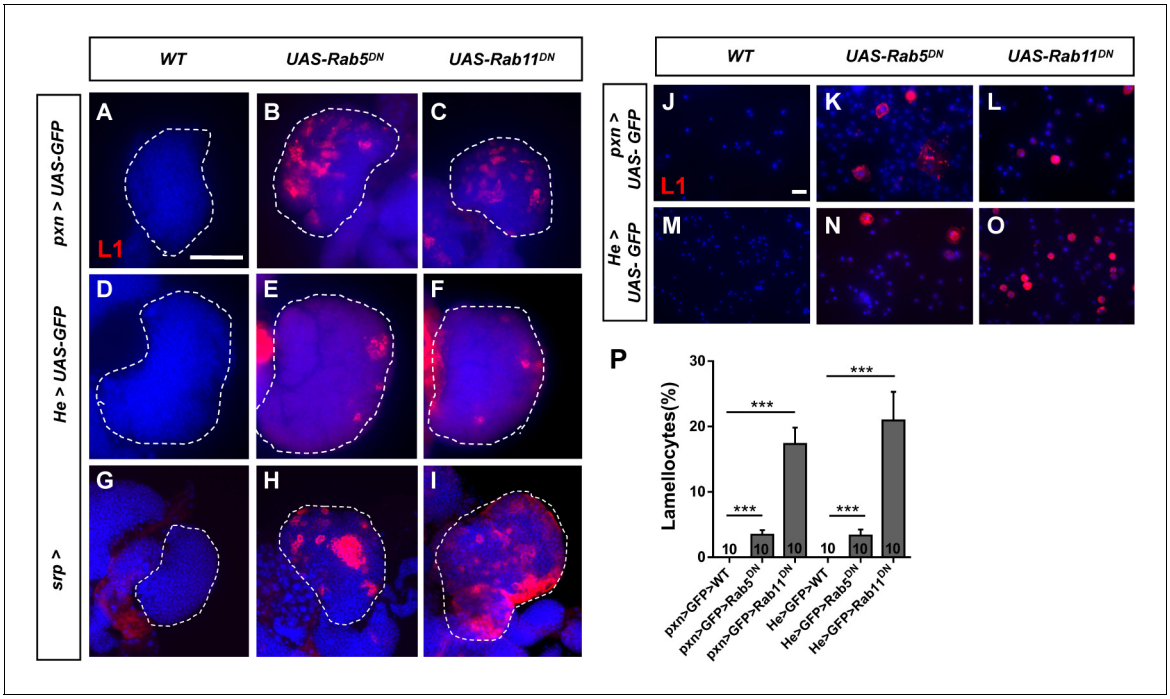

Figure 2—figure supplement 4. Inactivation of *Rab5/Rab11* with different hemocyte-specific Gal4 drivers resulted in massive lamellocyte formation. (**A–O**) Aberrant lamellocyte formation was observed in *pxn>UAS-GFP>UAS-Rab5/11^{DN}*, *He>UAS-GFP>UAS-Rab5/11^{DN}*, and *srp>UAS-Rab5/11^{DN}* lymph glands and in *pxn>UAS-GFP>UAS-Rab5/11^{DN}* and *He>UAS-GFP>UAS-Rab5/11^{DN}* circulating hemocytes. (**P**) The lamellocyte proportions from (**J–O**) are shown. Scale bars: 10 μm (hemocytes) and 50 μm (lymph glands). ***p<0.001 (one-way ANOVA).

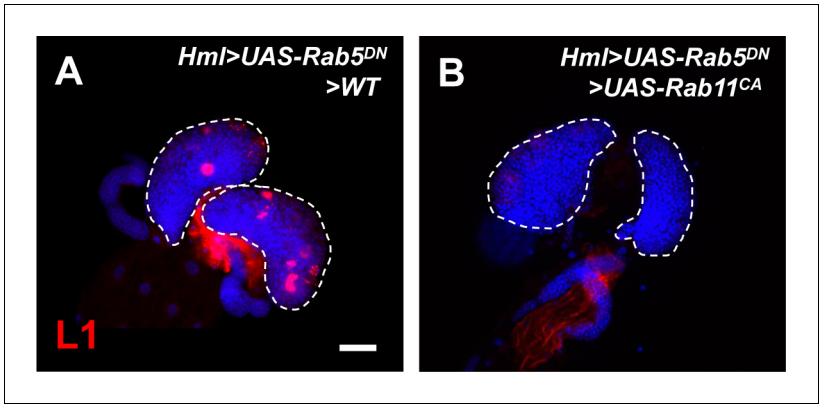

Figure 2—figure supplement 5. Active Rab11 GTPase activity could restore the aberrant lamellocyte differentiation in lymph glands after inhibition of *Rab5*. (**A and B**) Immunostaining of lamellocytes was performed with anti-L1 antibodies. The increased lamellocyte count was rescued in *Hml>UAS-Rab5^{DN}>UAS-Rab11^{CA}* lymph glands. Scale bar: 50 μm.

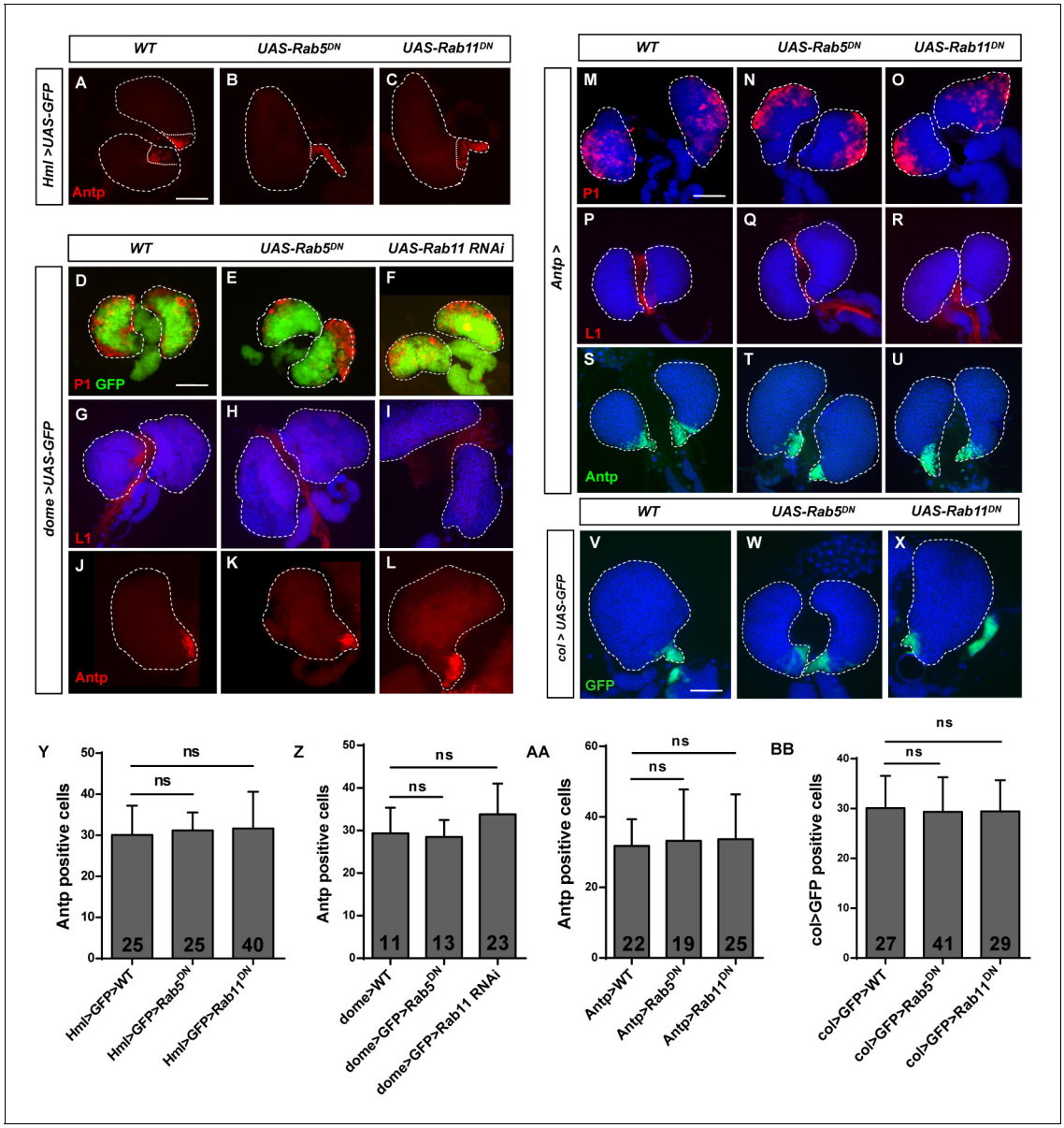

Figure 2—figure supplement 6. Analysis of the medullary zone (MZ) and posterior signaling center (PSC) upon the inactivation of *Rab5* or *Rab11*. PSC cells and the MZ were analyzed with anti-Antp antibodies or labeled with GFP after the inactivation of *Rab5* or *Rab11* using the *Hml-Gal4* (**A–C, Y**), *dome-Gal4* (**J–L, Z**), *Antp-Gal4* (**S–U, AA**), and *col-Gal4* (**V–X, BB**) drivers, respectively. The cortical zone (CZ) area and lamellocyte formation were determined with anti-P1 and anti-L1 antibodies after the inactivation of *Rab5* or *Rab11* using the *dome-Gal4* (**D–I**) and *Antp-Gal4* (**M–R**) drivers, respectively. Scale bar: 50 μm. ns, not significant (one-way ANOVA).

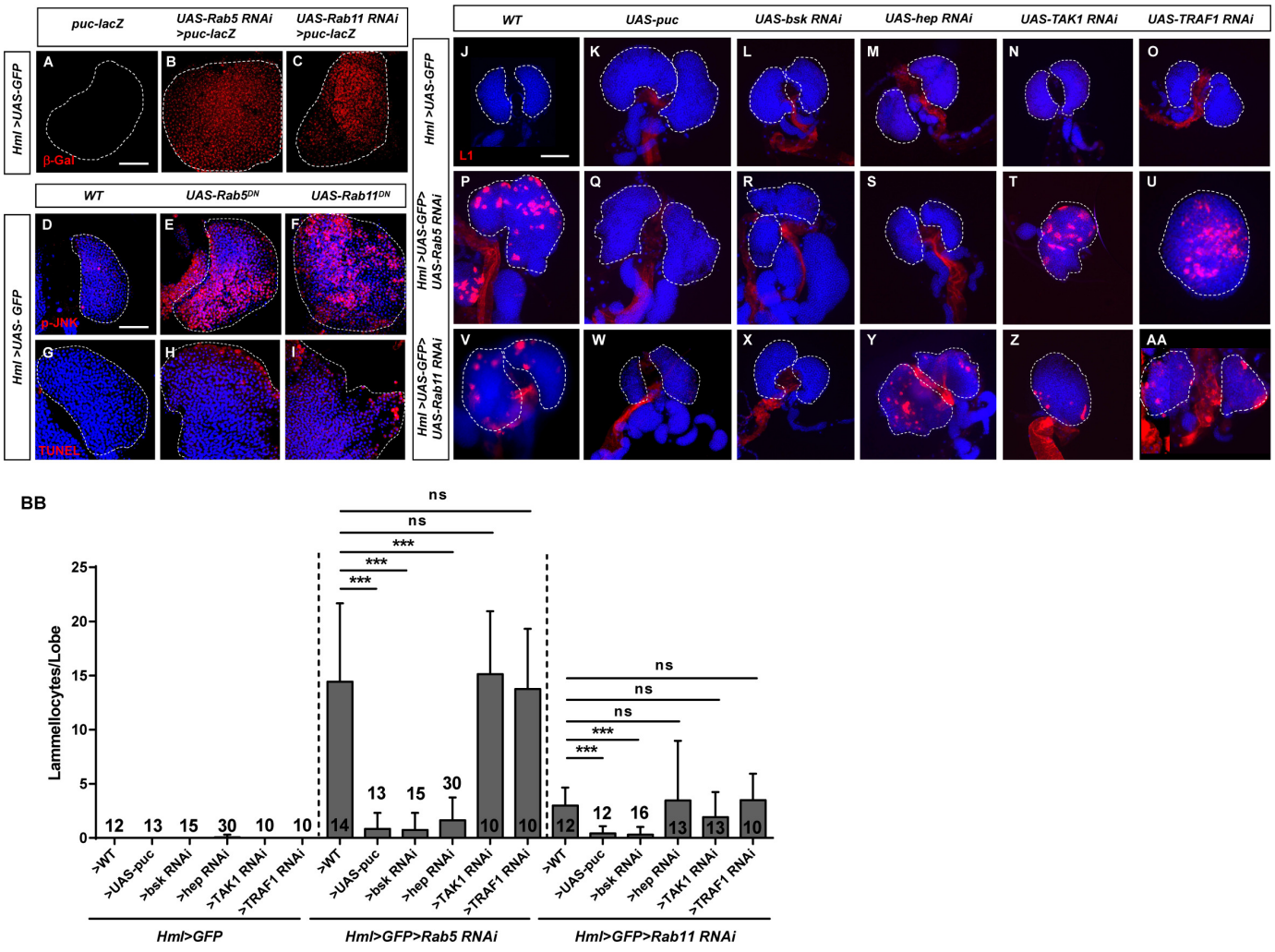

Figure 3. JNK signaling was activated upon *Rab5* or *Rab11* inactivation in the lymph gland. (**A–I**) The JNK pathway activity was elevated in lymph glands upon *Rab5* or *Rab11* inactivation, as elucidated by the monitoring of JNK signaling with *puc-lacZ* (**A–C**) and anti-p-JNK antibodies (**D–F**). Apoptotic cells in *Hml>UAS-GFP>UAS-Rab5^{DN}* and *Hml>UAS-GFP>UAS-Rab11^{DN}* lymph glands were detected by TUNEL assays (**G–I**). (**J–AA**) Immunostaining for L1 (red) showed that aberrant lamellocyte differentiation was rescued in *Hml>UAS-GFP>UAS-Rab5 RNAi>UAS-puc* (**Q**), *Hml>UAS-GFP>UAS-Rab11 RNAi>UAS-puc* (**W**), *Hml>UAS-GFP>UAS-Rab5 RNAi>UAS-bsk RNAi* (**R**), *Hml>UAS-GFP>UAS-Rab11 RNAi>UAS-bsk RNAi* (**X**), and *Hml>UAS-GFP>UAS-Rab5 RNAi>UAS-hep RNAi* (**S**) lymph glands. The quantifications for (**J–AA**) are shown in **BB**. Scale bar: 50 μm. ns, not significant; ***p<0.001 (one-way ANOVA).

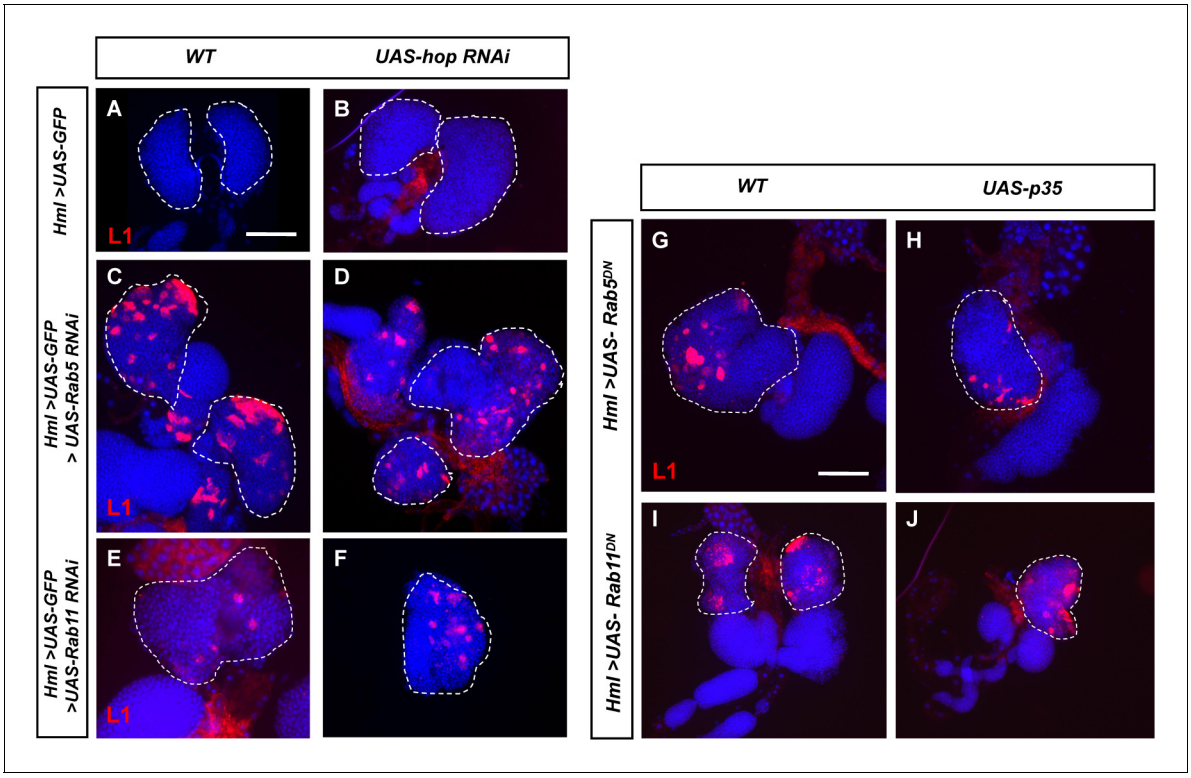

Figure 3—figure supplement 1. Knocking down *hop* or blocking apoptosis did not repress aberrant lamellocyte differentiation. Knocking down *hop* (**A–F**) or overexpressing *UAS-p35* (**G–J**) failed to repress the aberrant lamellocyte differentiation in *Hml>UAS-GFP>UAS-Rab5/11 RNAi* or *Hml>UAS-Rab5/11^{DN}* lymph glands. Scale bar: 50 μm.

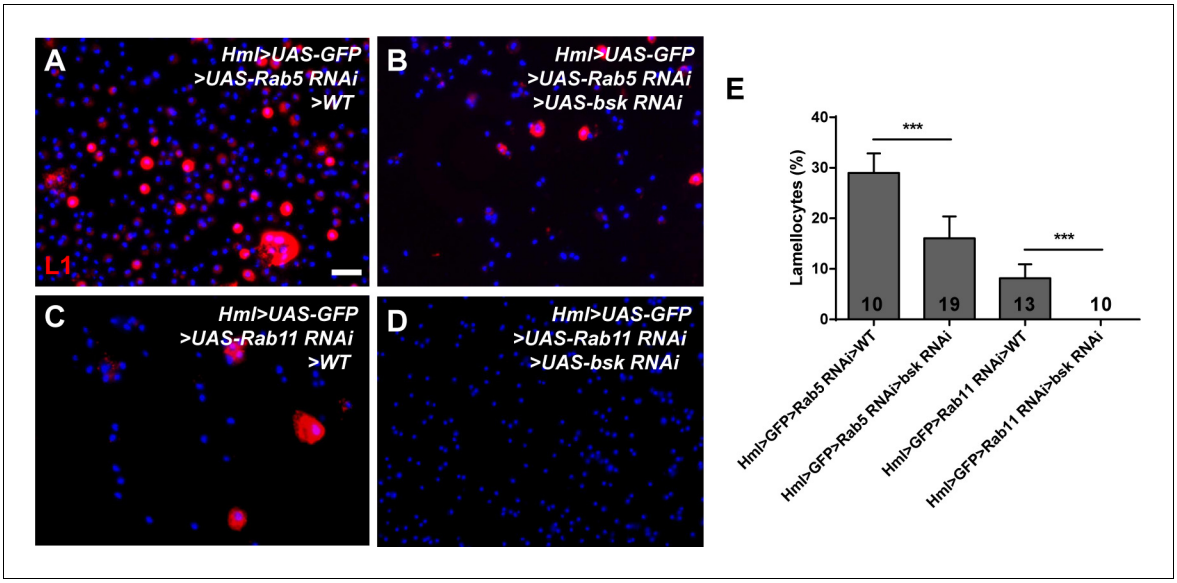

Figure 3—figure supplement 2. Knocking down *bsk* repressed aberrant lamellocyte differentiation in circulating hemocytes. (**A–D**) Knocking down *bsk* repressed the aberrant lamellocyte differentiation in *Hml>UAS-Rab5/11 RNAi* circulating hemocytes. Quantification of the lamellocyte count is shown in (**E**). Scale bar: 20 μm. ***p<0.001 (one-way ANOVA).

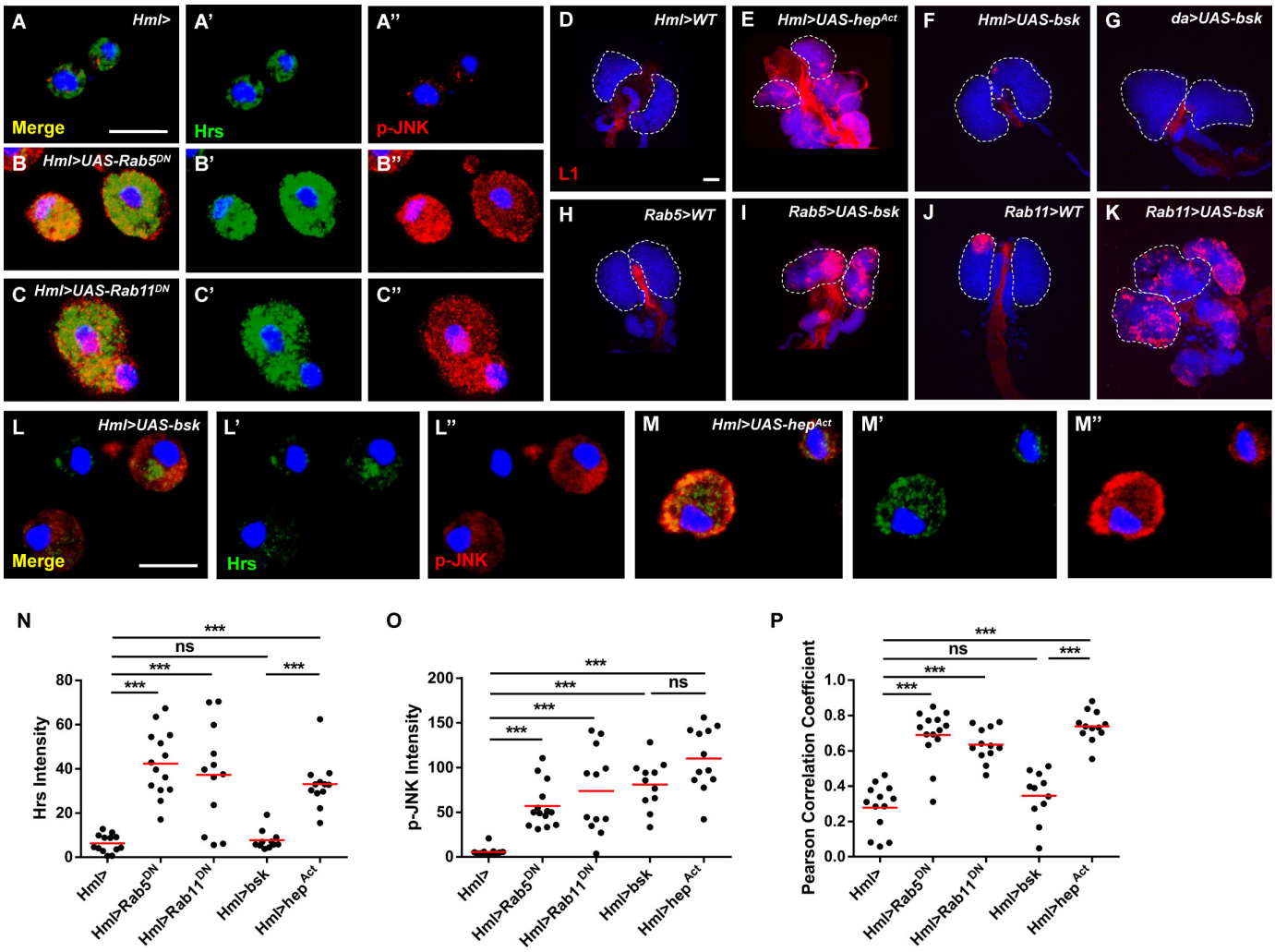

Figure 4. Inhibiting *Rab5* or *Rab11* induced high p-JNK levels in endosomes. (**A–C''**) An increased degree of Hrs (green) and p-JNK (red) colocalization was observed in *Hml>UAS-Rab5^{DN}* and *Hml>UAS-Rab11^{DN}* hemocytes. Merged images (Hrs+p-JNK+DAPI) are displayed in (**A–C**). (**D–K**) Massive lamellocyte formation was observed in lymph glands from *Hml>UAS-hep^{Act}* (**E**), *Rab5>UAS-bsk* (**I**), and *Rab11>UAS-bsk* (**K**) larvae. (**L–M''**) *Hml>UAS-hep^{Act}* hemocytes exhibited more Hrs (green) and p-JNK (red) colocalization than *Hml>UAS-bsk* hemocytes. The Hrs and p-JNK levels are shown in (**N**) and (**O**), respectively. (**P**) The colocalization degree between Hrs and p-JNK is displayed as the Pearson correlation coefficient, which was analyzed with the Colocalization Finder plugin from ImageJ. Scale bars: 50 μm (lymph glands) and 10 μm (hemocytes). ns, not significant; ***p<0.001 (one-way ANOVA).

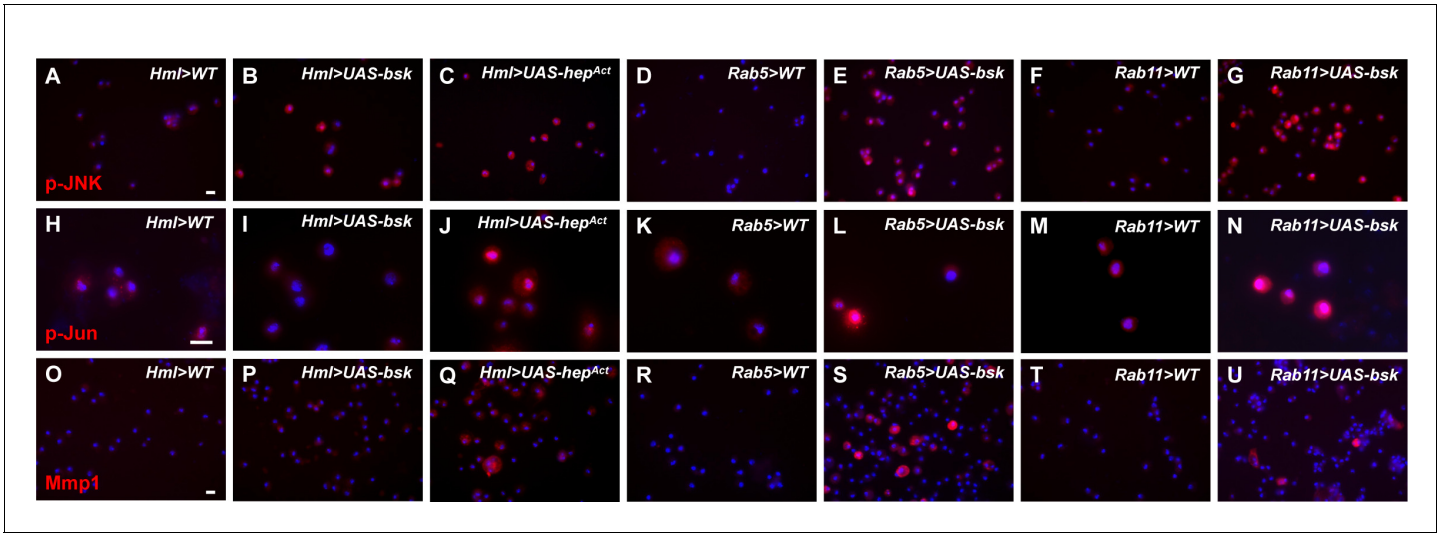

Figure 4—figure supplement 1. Analysis of the p-JNK, p-Jun, and Mmp1 levels in circulating hemocytes. (**A–U**) Circulating hemocytes were stained with antibodies against p-JNK (**A–G**), p-Jun (**H–N**), and Mmp1 (**O–U**). *Hml>UAS-hep^{Act}*, *Rab5>UAS-bsk*, and *Rab11>UAS-bsk* hemocytes showed elevated levels of p-JNK, p-Jun, and Mmp1, whereas only the p-JNK levels and not the p-Jun and Mmp1 levels were increased in *Hml>UAS-bsk* hemocytes. Scale bar: 10 μm.

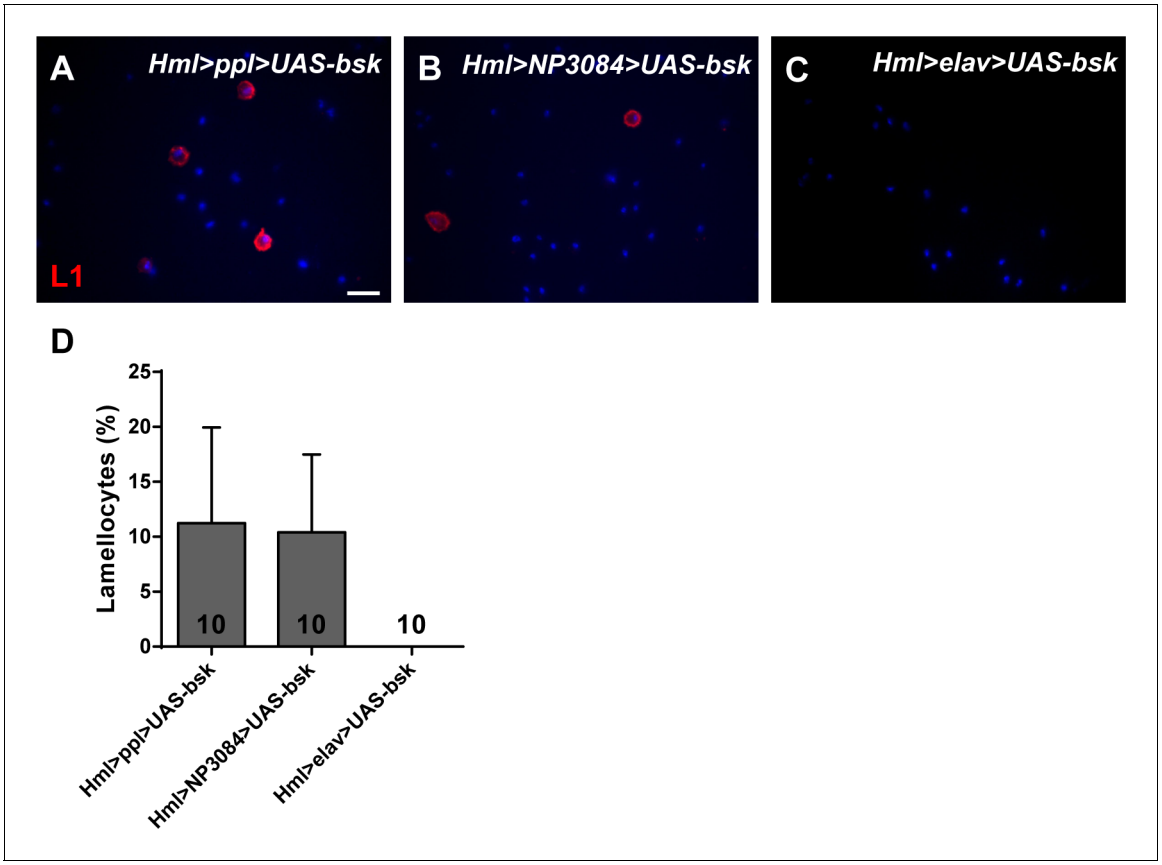

Figure 4—figure supplement 2. Overexpression of *bsk* in hemocytes and fat bodies or in hemocytes and the midgut simultaneously induced lamellocyte formation. (**A–D**) Hemocytes from *Hml>ppl>UAS-bsk*, *Hml>NP3084>UAS-bsk*, and *Hml>elav>UAS-bsk* larvae were stained with anti-L1 antibodies. The lamellocyte frequency in circulating hemocytes is shown in (**D**). Scale bar: 20 μm.

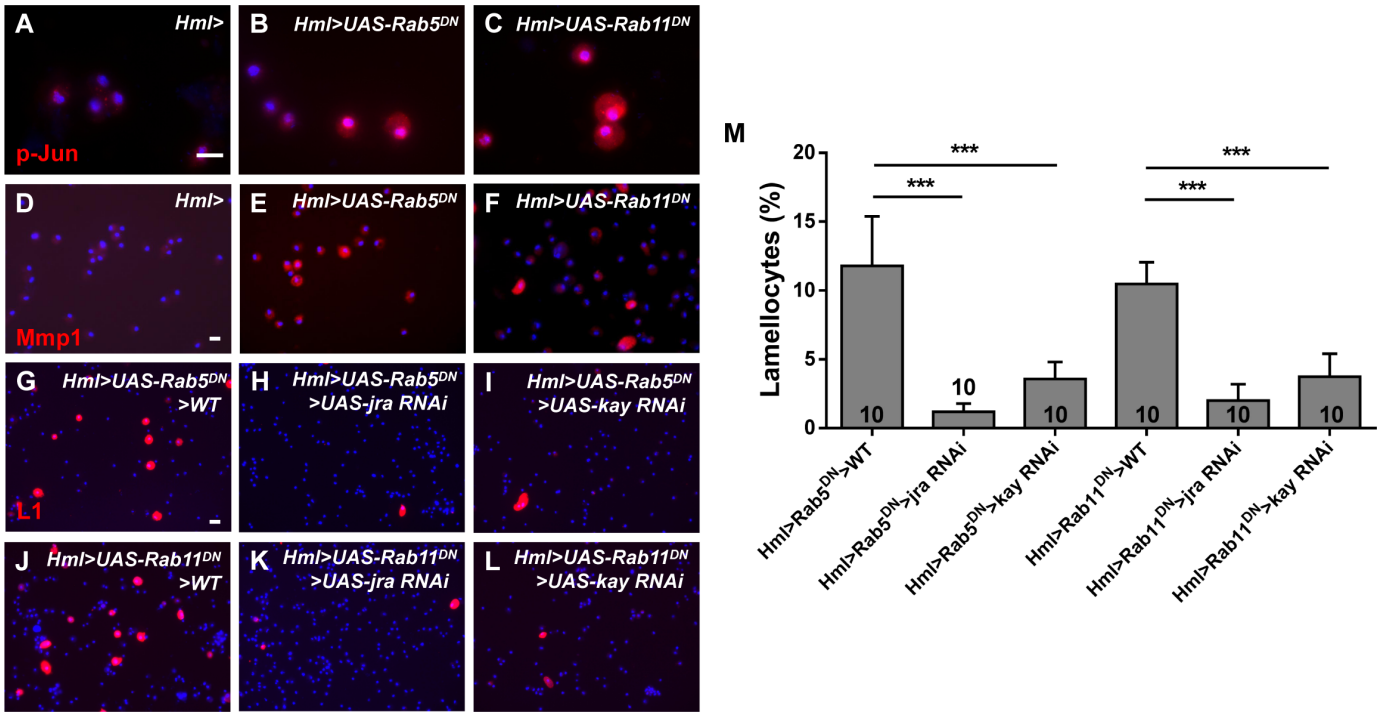

Figure 5. Inhibiting *Rab5* or *Rab11* in hemocytes increased the p-Jun and Mmp1 levels. (**A–F**) Immunostaining of circulating hemocytes showed that the levels of p-Jun (**A–C**) and Mmp1 (**D–F**) were increased after the inactivation of *Rab5* or *Rab11*. (**G–M**) The lamellocyte frequency, as analyzed by anti-L1 staining, was rescued in *Hml>UAS-Rab5^{DN}>UAS-jra/kay RNAi* and *Hml>UAS-Rab11^{DN}>UAS-jra/kay RNAi* circulating hemocytes. The percentage of L1-positive cells among total circulating hemocytes from (**G–L**) is shown in (**M**). Scale bar: 10 μm. ***p<0.001 (Student's *t*-test).

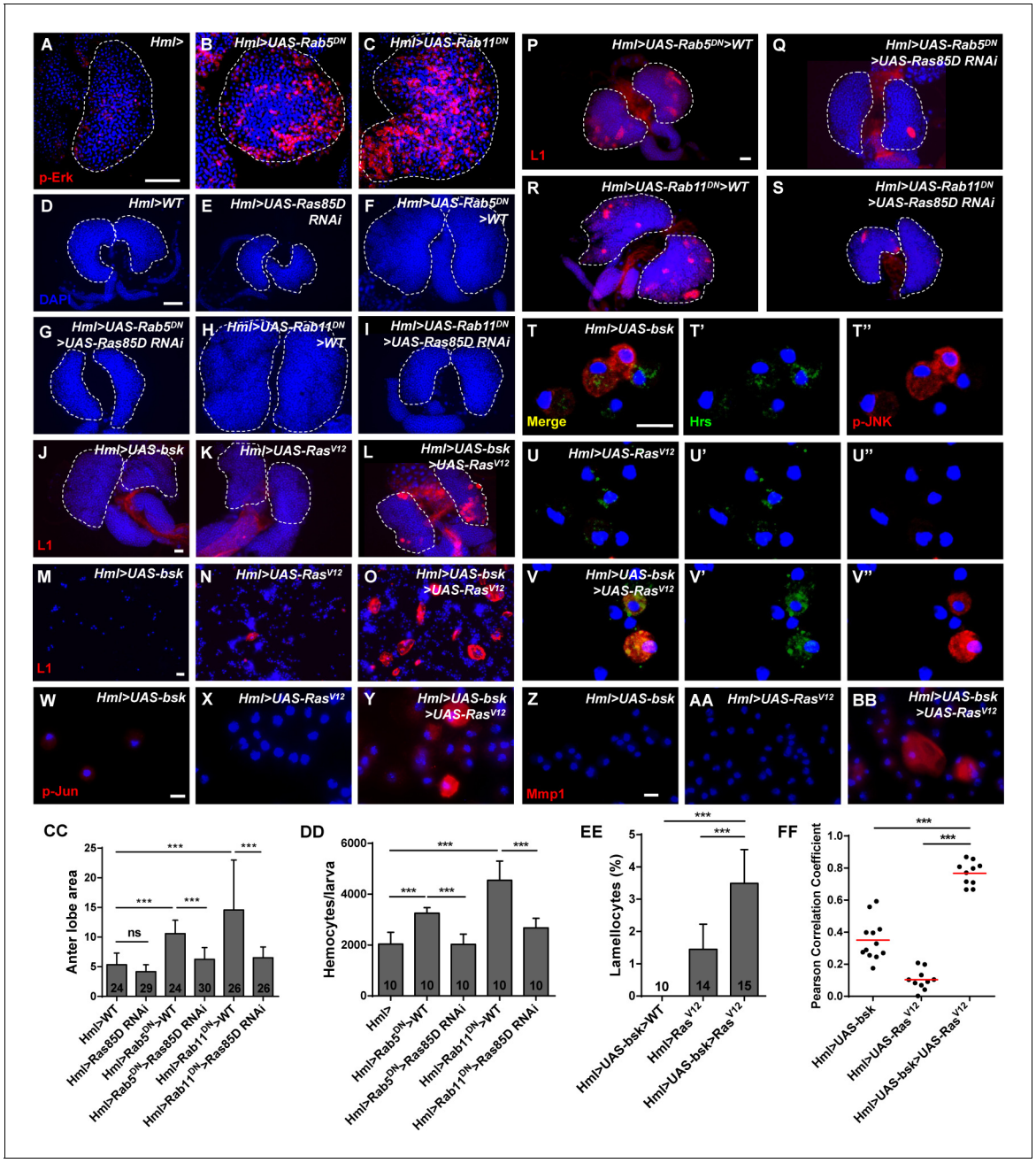

Figure 6. Ras/EGFR signaling was enhanced upon *Rab5* or *Rab11* inactivation. (**A–C**) Immunostaining of lymph glands showed high p-Erk (red) signals upon *Rab5* or *Rab11* inactivation. (**D–I**) Anterior lobe enlargement (visualized by DAPI staining) in *Hml>UAS-Rab5/11^{DN}* lymph glands was rescued after knockdown of *Ras85D*. (**CC**) Quantification of the anterior lobe area from (**D–I**). (**J–O**) The lamellocyte count was increased in lymph glands (**J–L**) and circulating hemocytes (**M–O**) when *bsk* and *Ras* were simultaneously overexpressed in the cortical zone (CZ). (**EE**) The lamellocyte frequency in circulating hemocytes from (**M–O**). (**P–S**) The increased lamellocyte count in lymph glands after *Rab5* or *Rab11* inactivation was rescued by the knockdown of *Ras* levels using *UAS-Ras85D RNAi*. (**T–BB**) Colocalization between Hrs (green) and p-JNK (red) (**T–V''**) and p-Jun and Mmp1 (**W–BB**) was increased in *Hml>UAS-bsk>UAS-Ras^{V12}* hemocytes compared with control hemocytes. The colocalization degrees are shown in (**FF**). (**DD**) Quantification of the circulating hemocyte counts in third instar larvae showed that the increased hemocyte count in *Hml>UAS-Rab5/11^{DN}* larvae was rescued by the downregulation of *Ras85D*. Scale bars: 50 μm (lymph glands) and 10 μm (hemocytes). ns, not significant; ***p<0.001 (one-way ANOVA).

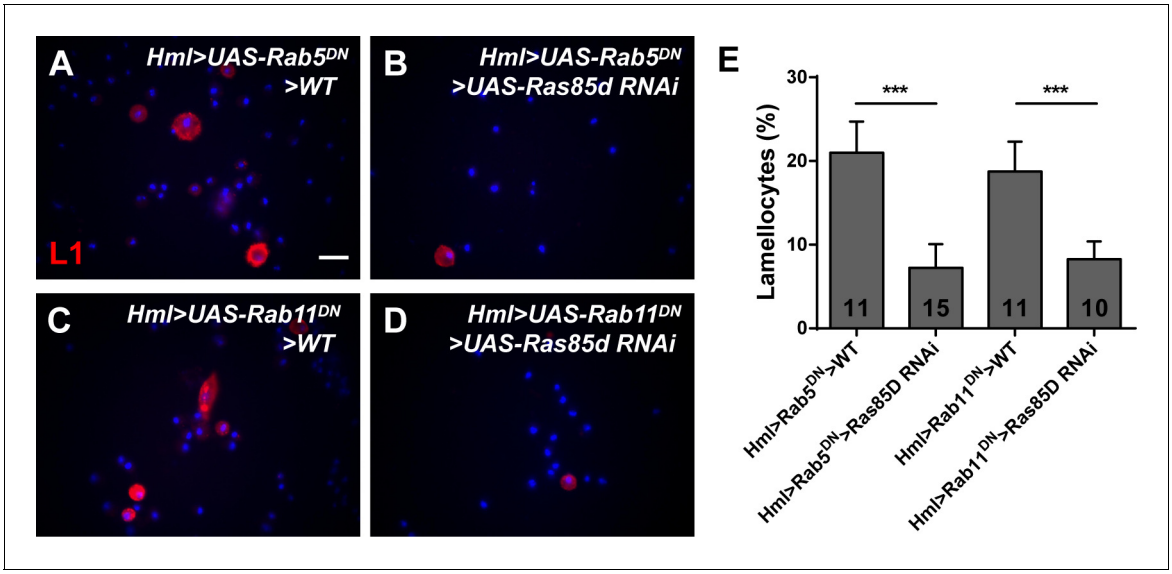

Figure 6—figure supplement 1. Knocking down *Ras85D* restored the aberrant lamellocyte differentiation in circulating hemocytes. (**A–D**) Knocking down *Ras85D* repressed the aberrant lamellocyte differentiation in *Hml>UAS-Rab5/11*^{DN} circulating hemocytes. (**E**) The lamellocyte frequency in circulating hemocytes. Scale bar: 20 μm. ***p<0.001 (one-way ANOVA).

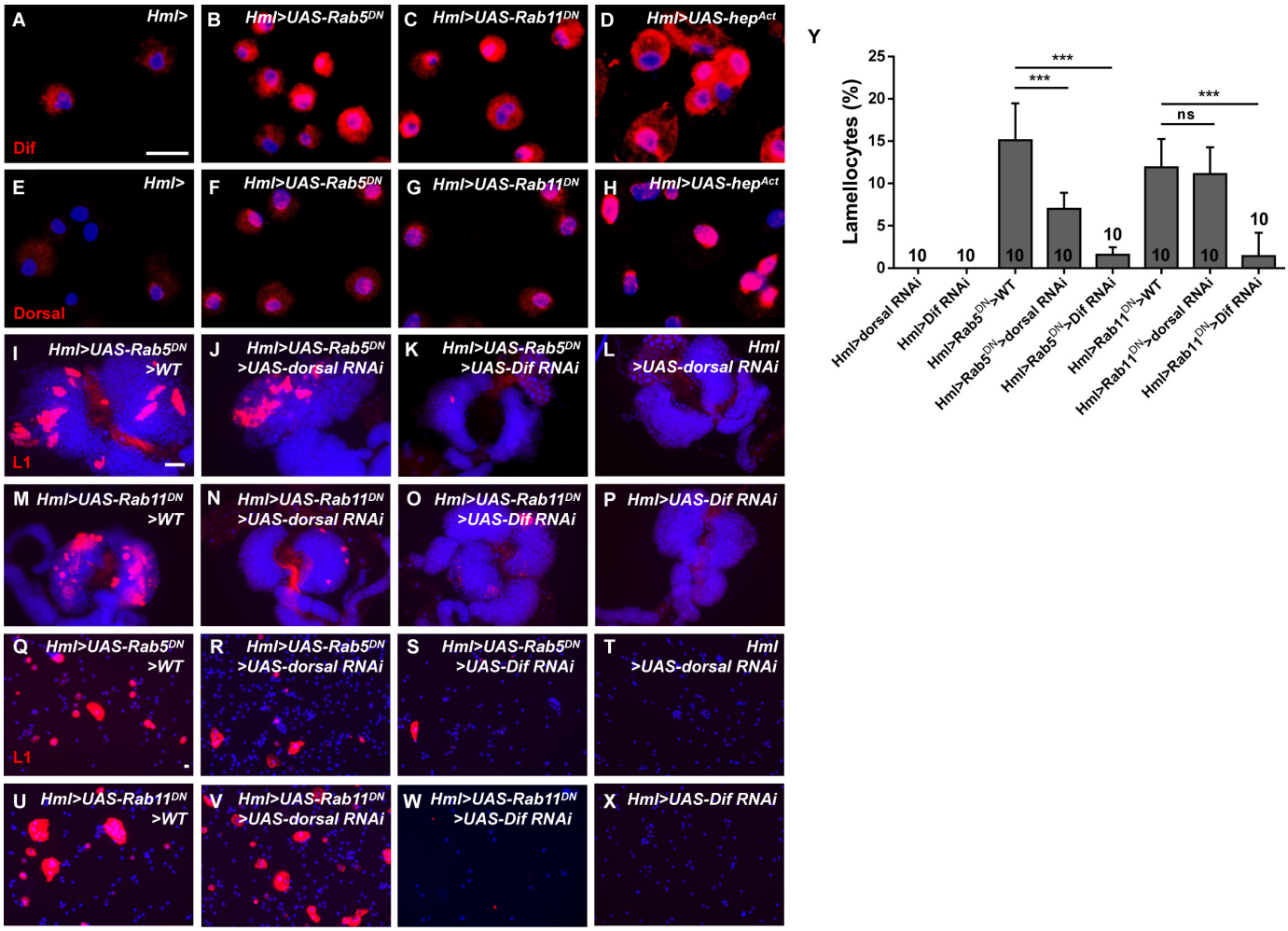

Figure 7. The Toll pathway was activated upon *Rab5* or *Rab11* inactivation. (**A–H**) Immunostaining of circulating hemocytes showed that Dif and Dorsal were activated in *Hml>UAS-Rab5/11^{DN}* (**B–C, F–G**) and *Hml>UAS-hep^{Act}* (**D, H**) hemocytes. (**I–X**) Detection of lamellocyte formation in hemocytes and lymph glands using anti-L1 antibodies (red) showed that *UAS-Dif RNAi* but not *UAS-dorsal RNAi* plays a significant role in restricting aberrant lamellocyte differentiation. The percentage of lamellocytes among circulating hemocytes is shown in (**Y**). Scale bars: 10 μm (hemocytes) and 50 μm (lymph glands). ns, not significant; ***p<0.001 (one-way ANONA).

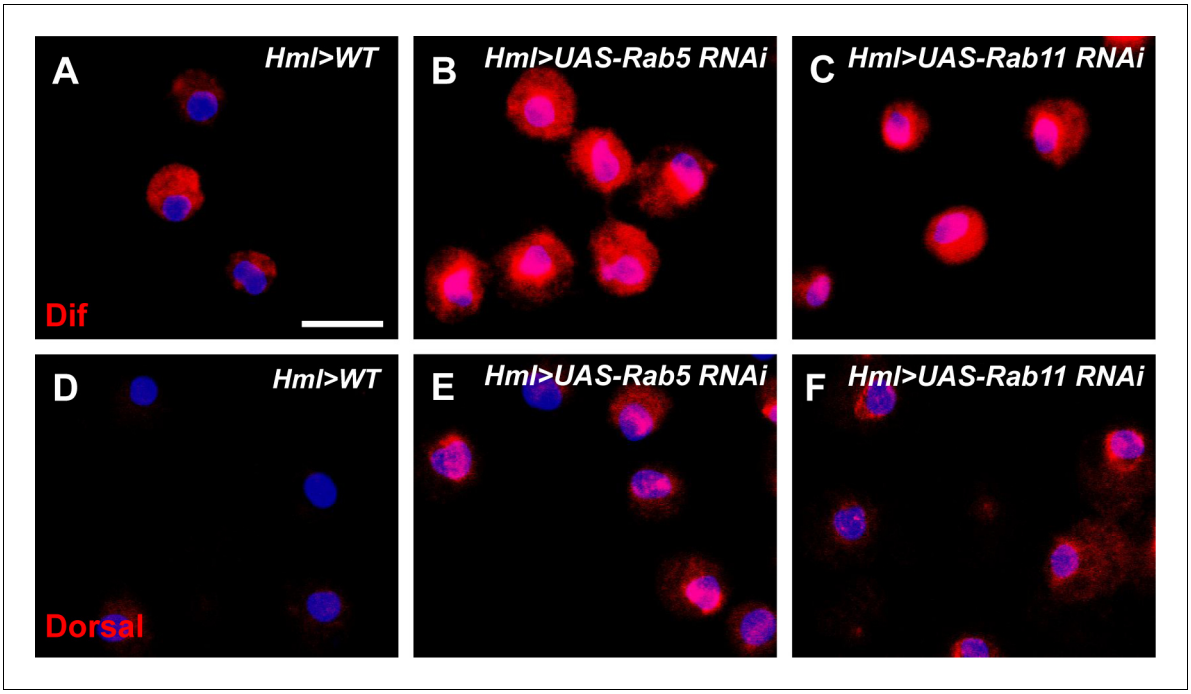

Figure 7—figure supplement 1. The Toll signaling pathway was activated upon the loss of *Rab5* or *Rab11*. The Dif (**A–C**) and Dorsal (**D–F**) levels were analyzed with immunostaining and found to be elevated in *Hml>UAS-Rab5 RNAi* and *Hml>UAS-Rab11 RNAi* hemocytes. Scale bar: 10 μm.

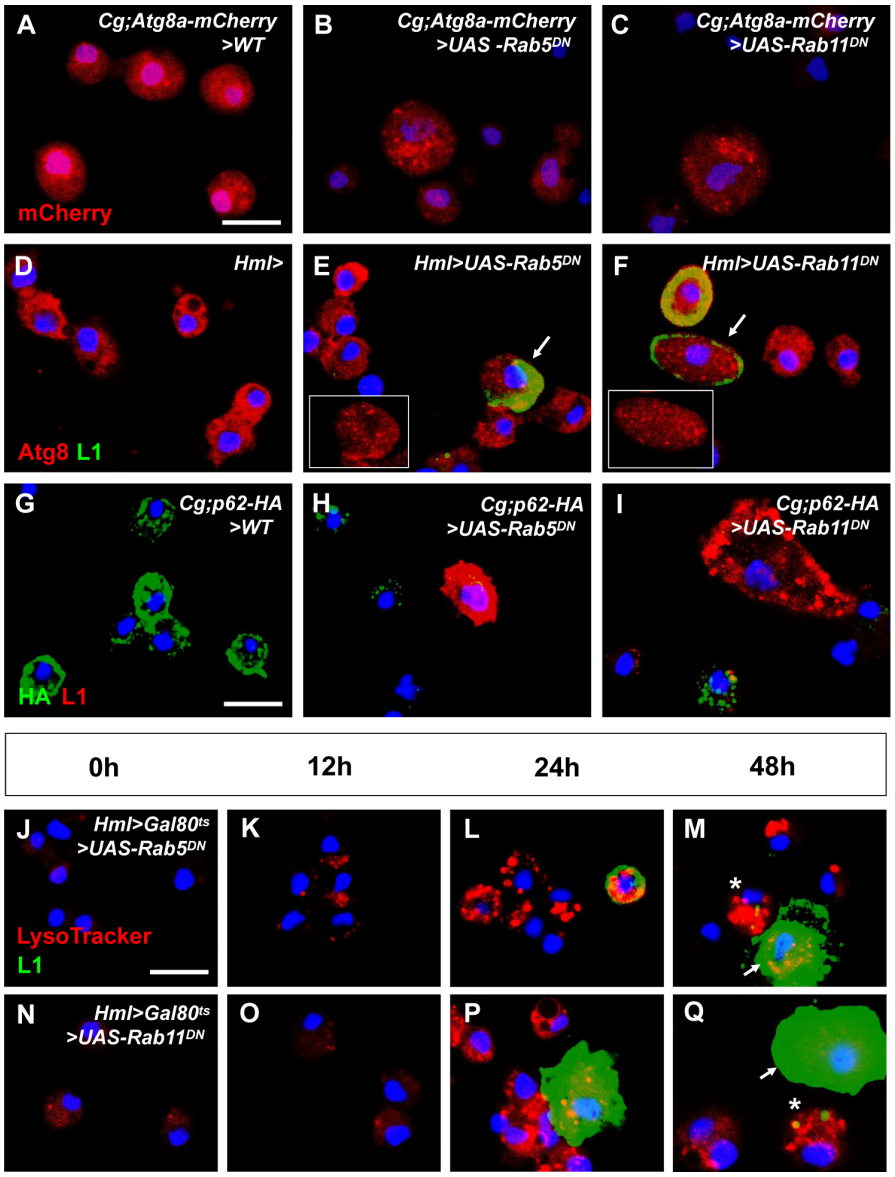

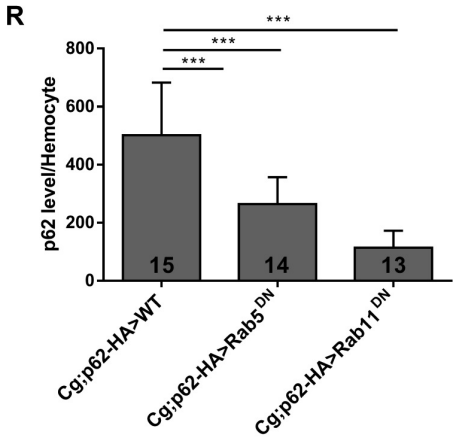

Figure 8. Loss of *Rab5* or *Rab11* activated autophagy in hemocytes. (**A–C**) Many autophagosomes were observed in *Cg;Atg8a-mCherry>UAS-Rab5^{DN}* and *Cg;Atg8a-mCherry>UAS-Rab11^{DN}* hemocytes. (**D–I**) Circulating hemocytes of *Hml-Gal4*, *Hml>UAS-Rab5^{DN}*, and *Hml>UAS-Rab11^{DN}* larvae were labeled with anti-Atg8 (red) and anti-L1 (green) antibodies, whereas those of *Cg;p62-HA>WT*, *Cg;p62-HA>UAS-Rab5^{DN}*, and *Cg;p62-HA>UAS-Rab11^{DN}* were labeled with anti-HA (green) and anti-L1 (red) antibodies (**G–I**). The arrows in (**E and F**) indicate lamellocytes with large numbers of autophagosomes. The average p62 levels per hemocyte as measured by evaluating HA fluorescence are shown in (**R**). (**J–Q**) The LysoTracker intensity (red) and lamellocyte differentiation (green) were examined in circulating hemocytes from *Hml>Gal80^{ts}>UAS-Rab5^{DN}* and *Hml>Gal80^{ts}>UAS-Rab11^{DN}* larvae after being shifted to 29°C for 0 hr, 12 hr, 24 hr, and 48 hr. In (**M**) and (**Q**), the asterisks indicate 'intermediates', and the arrows indicate 'mature lamellocytes'. Scale bar: 10 μm. ***p<0.001 (one-way ANOVA).

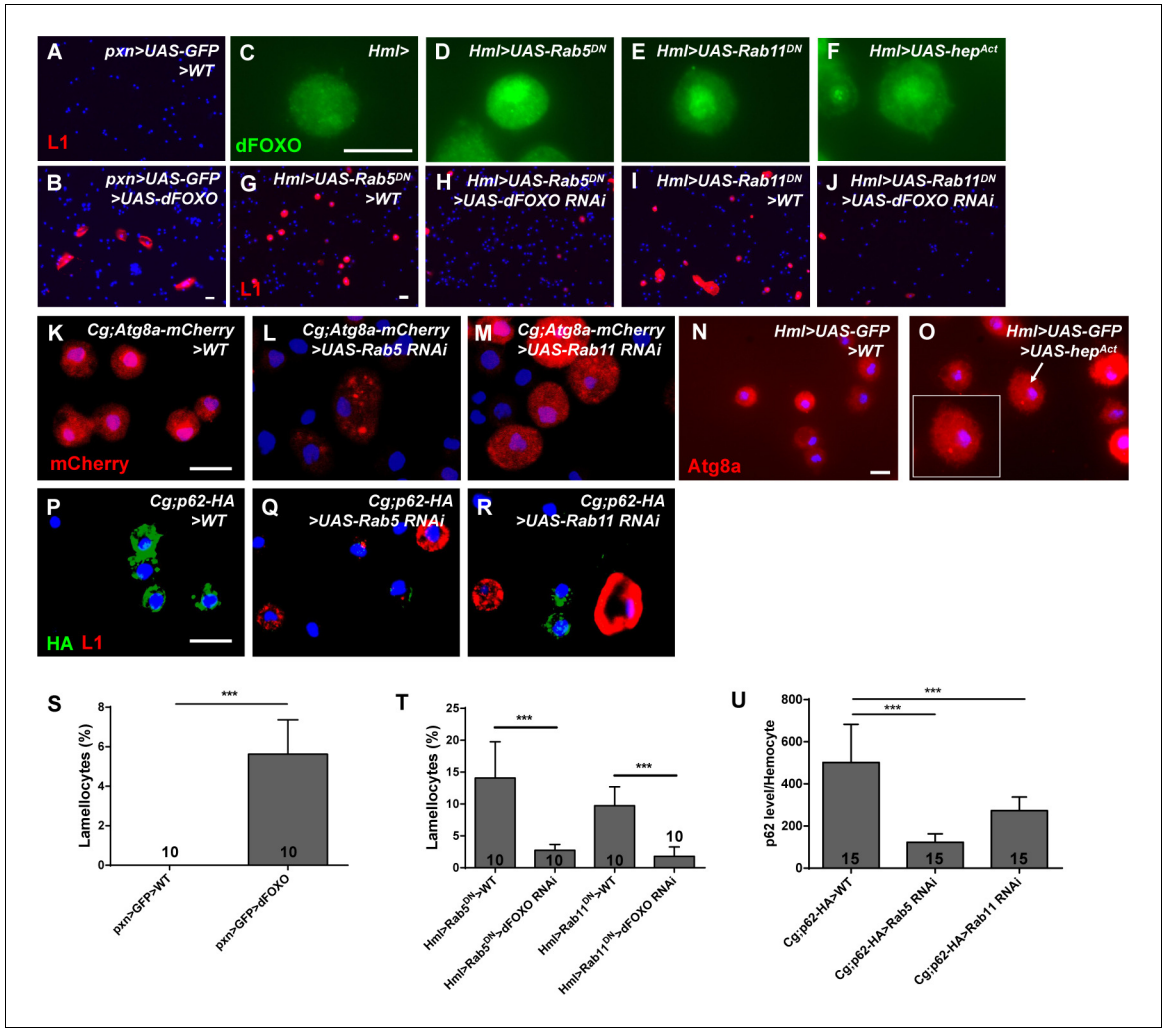

Figure 8—figure supplement 1. The dFOXO levels and autophagy activity were enhanced after the inactivation of *Rab5* or *Rab11* in hemocytes. (**A and B**) Overexpression of *dFOXO* in hemocytes using *pxn>GFP* induced lamellocyte formation. (**C–F**) The dFOXO (green) levels were increased in circulating hemocytes from *Hml>UAS-Rab5^{DN}*, *Hml>UAS-Rab11^{DN}*, and *Hml>UAS-hep^{Act}* larvae. (**G–J**) Rescue assays were performed with anti-L1 antibodies in lymph glands. Knockdown of *dFOXO* rescued the lamellocyte count among *Hml>UAS-Rab5/11^{DN}* circulating hemocytes. The lamellocyte fraction is shown in (**S and T**). Autophagosomes were formed in *Cg;Atg8a-mCherry>UAS-Rab5/11 RNAi* hemocytes, as shown by mCherry fluorescence (**K–M**), and in *Hml>UAS-GFP>UAS-hep^{Act}* hemocytes, as analyzed with anti-Atg8 antibodies (**N and O**). The arrow indicates cells with autophagosomes. (**P–R**) *Cg;p62-HA>WT*, *Cg;p62-HA>UAS-Rab5 RNAi*, and *Cg;p62-HA>UAS-Rab11 RNAi* hemocytes were labeled with anti-HA (green) and anti-L1 (red) antibodies. The average p62 levels per hemocyte were measured by HA fluorescence and are shown in (**U**). Scale bar: 10 μm. ***p<0.001 (Student's *t*-test for [**S and T**]; one-way ANOVA for [**U**]).

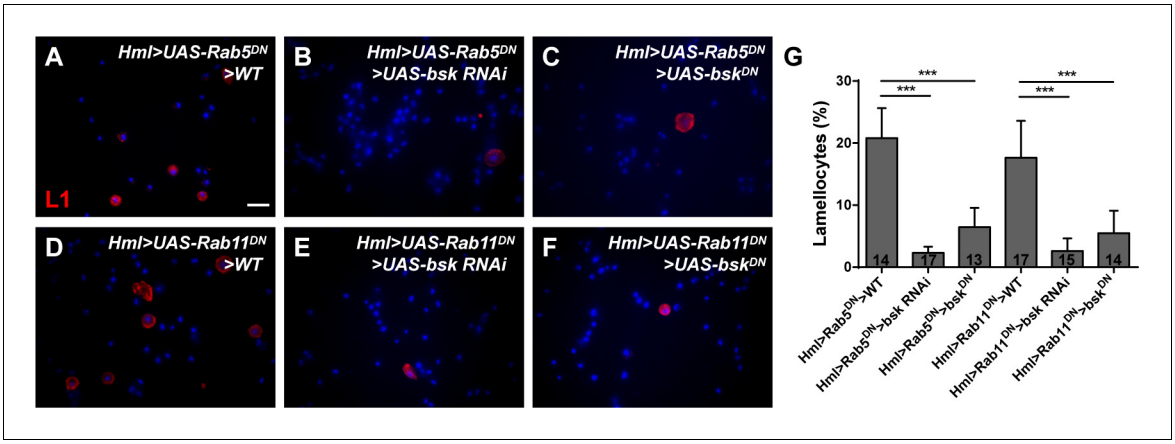

Figure 8—figure supplement 2. Repressing JNK signaling restored the increased lamellocyte count in *Hml>UAS-Rab5/11^{DN}* larvae. (**A–F**) The increased lamellocyte counts were restored in *Hml>UAS-Rab5/11^{DN}>UAS-bsk RNAi* (**B, E**) and *Hml>UAS-Rab5/11^{DN}>UAS-bsk^{DN}* (**C, F**) circulating hemocytes. The quantification of lamellocytes is shown in (**G**). Scale bar: 20 μm. ***p<0.001 (one-way ANOVA).

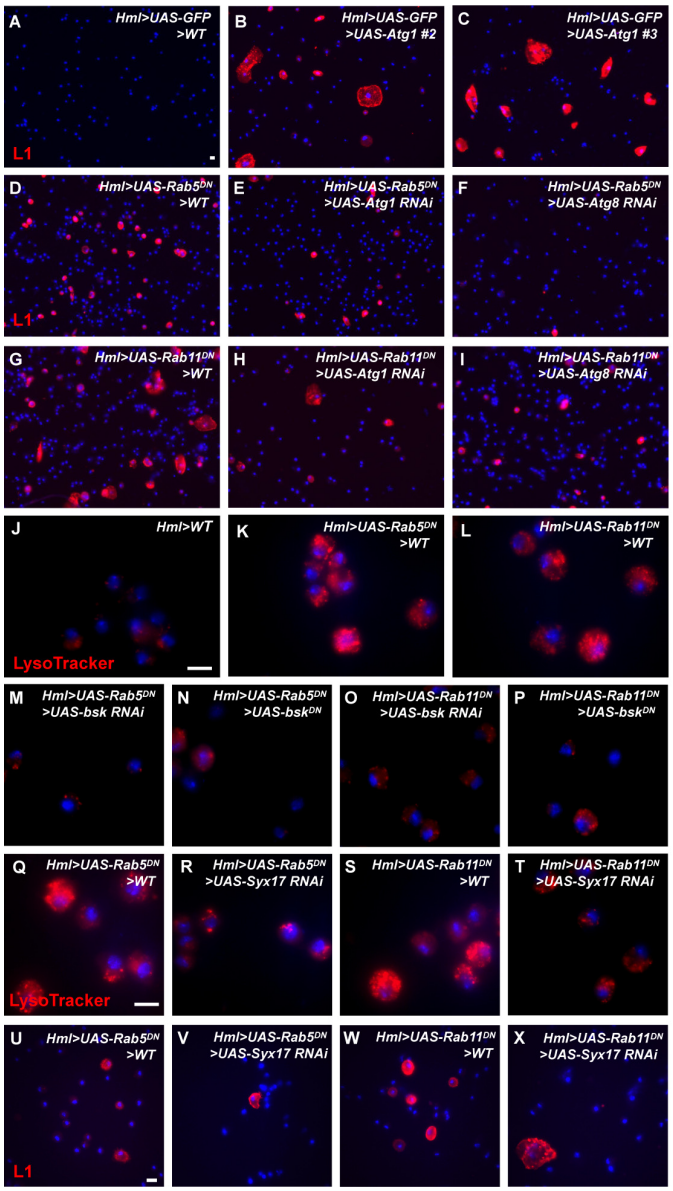

Figure 9. The lamellocyte formation upon the loss of *Rab5* or *Rab11* was autophagy-dependent. (**A–I, U–X**) The lamellocyte count was determined in circulating hemocytes by anti-L1 immunostaining. Overexpression of *Atg1* in two sources of *UAS-Atg1* flies resulted in massive lamellocyte production (**A–C**). In addition, knocking down *Atg1* (**E, H**), *Atg8* (**F, I**), *or Syx17* (**V, X**) in *Hml>UAS-Rab5/11^{DN}* larvae suppressed the increase in the lamellocyte count. (**Y–BB**) The lamellocyte numbers were quantified. (**J–T**) LysoTracker staining in circulating hemocytes showed that the increased LysoTracker intensity was suppressed in *Hml>UAS-Rab5/Rab11^{DN}>UAS-bsk RNAi*, *Hml>UAS-Rab5/Rab11^{DN}>UAS-bsk^{DN}*, and *Hml>UAS-Rab5/Rab11^{DN}>UAS-Syx17 RNAi* hemocytes. Scale bar: 10 μm. ***p<0.001 (one-way ANOVA).

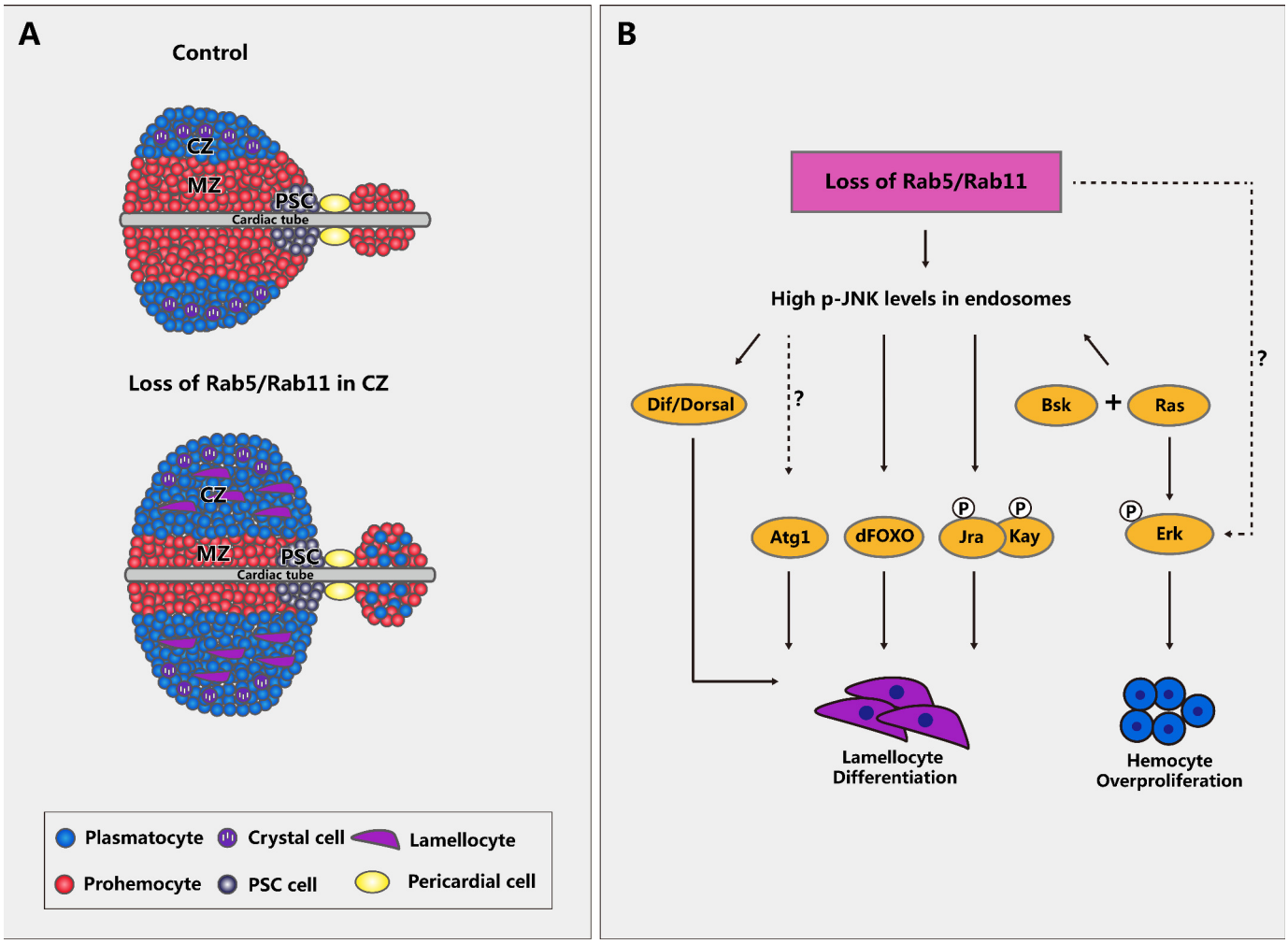

Figure 10. Schematic diagram of lymph gland morphology and the regulatory network of signaling pathways upon *Rab5*/*Rab11* inactivation. (**A**) Schematic diagram of lymph glands from control and *Rab5*/*Rab11*-deficient third instar larvae. When *Rab5* or *Rab11* was downregulated in the cortical zone (CZ), the formation of many premature hemocytes and lamellocytes was induced in the anterior and posterior lobes, whereas the medullary zone (MZ) area was decreased. Different cell types are represented by different colors and shapes. (**B**) Inhibiting *Rab5* or *Rab11* led to high p-JNK levels in endosomes. Next, activation of multiple signaling pathways, including JNK, Ras/EGFR, and Toll, ultimately contributed to lamellocyte differentiation and cell overproliferation.